Steady-State and Picosecond Laser Fluorescence Studies of Nonradiative Pathways in Tricarbocyanine Dyes: Implications to the Design of Near-IR Fluorochromes with High Fluorescence Efficiencies

Steven A. Soper* and Quincy L. Mattingly

Contribution from the Department of Chemistry, Louisiana State University, Baton Rouge, Louisiana 70803-1804

Received November 8, 1993®

Abstract: In order to rationally design probes appropriate for sensitive near-infrared (NIR) applications, fluorescence studies of two representative tricarbocyanine NIR dyes, IR-125 and IR-132, were undertaken to evaluate solvent-dependent and independent nonradiative relaxation pathways. The fluorescence quantum yields, lifetimes, and the radiative and nonradiative rates in aqueous solvents, organic alcohols, and binary mixtures of water/methanol were measured using steady-state and picosecond laser techniques. In addition, organized media and solvent viscosity effects on the NIR dyes' photophysical properties were investigated. The quantum yields were less than 15% with subnanosecond lifetimes in all solvent systems investigated with severely reduced quantum yields and lifetimes in aqueous solvents when compared to those in the neat organic alcohols. Inspection of the absorption spectra indicated extensive ground-state aggregation for IR-132 in aqueous solvents, while IR-125 showed little evidence of aggregation. The fluorescence lifetimes for both dyes demonstrated negligible dependence on solution viscosity, indicating that photoisomerization is not a major nonradiative path for these tricarbocyanine dyes. Linear free energy plots of the nonradiative rates (k_{nr}) and the solvent's $E_T(30)$ value (parameter indicative of solvent polarity and hydrogen bond donating ability) showed a linear relationship in the neat alcohols and H_2O/methanol binary mixtures, with larger solvent $E_T(30)$ values yielding larger nonradiative rates. Inverse linear relationships with poor correlations were found between the solvent's nucleophilicity and the nonradiative rates. The addition of certain surfactants, such as sodium dodecyl sulfate (anionic), and *tert*-octylphenoxy polyethoxyethanol (nonionic) above their critical micelle concentrations improved the photophysical properties of these dyes when compared to the pure aqueous solvents. Internal conversion resulting from the small electronic energy difference between the ground and first excited singlet, a nonrigid molecular structure giving rise to many vibrational degrees of freedom and distortion of the molecule from planarity, was surmised to be the major nonradiative manifold of the singlet excited state. A solvent-dependent nonradiative rate was also discovered, with the efficiency of this process determined by the hydrogen bond donating strength and/or polarity of the solvent. The photophysical results warrant consideration of the following constraints in the design of new fluorochromes requiring high fluorescence efficiencies appropriate for the NIR: inclusion of charged functionalities on the dye to prevent aggregation; exclusion of heavy atoms within the dye structure; structural reinforcement within the polymethine chain to reduce the rate of internal conversion; and inclusion of organized media in the aqueous environment when appropriate to shield the dye from the strong hydrogen bond donating strength and/or polarity of the interstitial solution.

Introduction

There is a growing interest in adapting applications to use near-infrared (NIR) fluorescence in chemistry[1] and biochemistry[2] due to small matrix interferences generated by impurities which can limit the sensitivity of the measurement. Recently, our group has reported detection sensitivity at the single molecule level in the NIR using pulsed-laser excitation and time-gated detection for the NIR fluorescent dye IR-132 in methanol.[3] The single molecule detection efficiency for the NIR dye showed a significant improvement over that observed for the visible dye, rhodamine 6G (R6G), even though the NIR dye possessed a smaller quantum yield, shorter fluorescence lifetime, and poorer photochemical stability. The improvement in detection efficiency resulted primarily from the low background arising from fluorescent impurities in the solvent blank when using NIR excitation.

A major bottleneck in the complete utilization of NIR fluorescence for many applications is the limited number of fluorochromes with high fluorescence efficiencies appropriate for this region of the spectrum. A group of dyes typically used in NIR fluorescence applications are the di- and tricarbocyanines. Early work on the photophysics was motivated by the use of these dyes as photosensitizers and a gain media or saturable absorbers in synchronously mode-locked dye lasers. Several groups have synthetically prepared NIR carbocyanine dyes possessing functional groups which form conjugates with several different classes of molecules, permitting their potential use as fluorescent probes for the analysis of DNA, lipids, peptides, and proteins.[4-6] The carbocyanine dyes consist of aromatic or heteroaromatic ring

* Author to whom correspondence should be addressed.

® Abstract published in *Advance ACS Abstracts*, April 1, 1994.

(1) (a) Imasaka, T.; Yoshitake, A.; Ishibashi, N. *Anal. Chem.* **1984**, *56*, 1077–1079. (b) Imasaka, T.; Yoshitake, A.; Hirata, K.; Kawabata, Y.; Ishibashi, N. *Anal. Chem.* **1985**, *57*, 947–949. (c) Sauda, K.; Imasaka, T.; Ishibashi, N. *Anal. Chem.* **1986**, *187*, 353–356. (d) Imasaka, T.; Tsukamoto, A.; Ishibashi, N. *Anal. Chem.* **1989**, *61*, 2285–2288. (e) Imasaka, T.; Ishibashi, N. *Anal. Chem.* **1990**, *62*, 363A–371A. (f) Roberson, M. A.; Andrews-Wilberforce, D.; Norris, D.; Patonay, G. *Anal. Lett.* **1990**, *23*, 719–734. (g) Patonay, G.; Antoine, M. D. *Anal. Chem.* **1991**, *63*, 321A–327A. (h) Patonay, G.; Antoine, M.; Devanathan, S.; Strekowski, L. *Appl. Spectrosc.* **1991**, *45*, 457–461. (i) Zen, J.-Y.; Patonay, G. *Anal. Chem.* **1991**, *63*, 2934–2938. (j) Higashijima, T.; Fuchigami, T.; Imasaka, T.; Ishibashi, N. *Anal. Chem.* **1992**, *64*, 711–714.

(2) (a) Wolf, D. *Biochemistry* **1985**, *24*, 582–586. (b) Packard, B.; Wolf, D. *Biochemistry* **1985**, *24*, 5176–5181. Hollins, B.; Noe, B.; Henderson, J. *Clin. Chem.* **1987**, *33*, 765–768. (c) O'Reilly, T.; MacMathuna, P.; Keeling, P.; Feely, J. *J. Chromatogr.* **1987**, *417*, 190–196. (d) Awni, W.; Bakker, L. *Clin. Chem.* **1989**, *35*, 2124–2126. (e) Reers, M.; Smith, T.; Chen, L. *Biochemistry* **1991**, *30*, 4480–4486.

(3) Soper, S.; Mattingly, Q.; Vegunta, P. *Anal. Chem.* **1993**, *65*, 740–747.

(4) Bello, K. A.; Cheng, L.; Griffiths, J. *J. Chem. Soc., Perkin Trans.* **1987**, 815–818.

0002-7863/94/1516-3744$04.50/0 © 1994 American Chemical Society

structures linked by a polymethine chain possessing conjugated carbon/carbon double bonds. A bathochromic shift results as the length of the polymethine chain is increased. The carbocyanine dye 3,3′-diethylthiadicarbocyanine iodide (DTDCI) exhibits an absorption maximum at 662 nm in dimethyl sulfoxide (DMSO), while the dye 3,3′-diethylthiatricarbocyanine iodide (DTTCI) possesses an absorption maximum at 772 nm.

The difficulties associated with the use of these dyes are the small fluorescence quantum yields they exhibit when compared to many visible fluorescent dyes and the major changes which occur in the spectroscopic properties when placed in aqueous solvents, severely limiting their use in critical applications. Some of these changes include extensive ground-state aggregation and solvent-dependent photophysics, with aqueous solvents or other high-polarity solvents resulting in reduced fluorescence quantum efficiencies and shorter fluorescence lifetimes.[7,8] For example, the dye 4,5-benzindopentacarbocyanine has a shorter fluorescence lifetime in the more polar solvent ethanol when compared to that in 1,2-dichloroethane (DCE).[9] The nucleophilic properties of the solvent were concluded to be the solvent parameter responsible for the observed photophysics. Since ethanol is a better nucleophile than DCE, ethanol is effective at solvating the excited state of the dye, decreasing the energy of the excited state and resulting in increased nonradiative energy transfer between various solvated forms of the dye.[10]

Internal conversion has been shown to be a major nonradiative pathway in polymethine dyes due primarily to the nonplanar structure of the molecule arising from a conformationally "loose" polymethine chain linking the heteroaromatic fragments, with the efficiency of this deactivation pathway related, in part, to the degree of steric hindrance between the heteroaromatic fragments. Increases in the length of the polymethine chain for a series of structurally similar dyes have been shown to result in increases in the fluorescence properties.[11-13] In addition, restricting the molecule to a planar conformation through covalent bridging of the heteroaromatic fragments can dramatically reduce the rate of this internal conversion process.[14] The internal conversion deactivation pathway has also been demonstrated to exhibit a time dependency. The time-dependent rate of internal conversion arises from partial rotation of the quinolyl fragments during the excited-state lifetime. The fluorescence lifetime of the dye 3,3′-diethyl-4,5,4′,5′-dibenzthiacarbocyanine bromide was shown to be shorter in methanol when compared to that in ethanol, and the decrease in the lifetime was attributed to the smaller viscosity of methanol.[15] The increased viscosity of the solution inhibits the conformational rotation of the heteroaromatic fragments during the excited-state lifetime, giving rise to a longer fluorescence lifetime and a time-dependent rate of internal conversion.[15,16]

Another proposed path for nonradiative deactivation in carbocyanine and dicarbocyanine dyes is cis/trans photoisomerization within the polymethine chain.[17-21] Photoisomerization in several di- and tricarbocyanines has been documented through observation of the transient absorption spectra originating from the photoisomer,[22] a second component in the fluorescence decay profile,[15] and large viscosity effects on the fluorescence lifetime.[23-25]

Although di- and tricarbocyanine dyes typically demonstrate poor fluorescence properties in aqueous solvents, the problem can be circumvented to a certain extent by the addition of surfactants above their critical micelle concentration (CMC) to the aqueous solvent.[26-28] The enhanced fluorescence properties demonstrated by many carbocyanine dyes in organized media was believed to result from the microviscosity of the hydrophobic core associated with the micelle, which is greater than that of the interstitial solution (microviscosity of SDS micelles is reported to be approximately 15–30 cP[29]). The increased viscous drag associated with the interior of the micelle inhibits the conformational change necessary for isomerization to occur during the excited-state lifetime of the dye.[28]

In order to rationally design new tricarbocyanine dyes with favorable fluorescence properties in aqueous and nonaqueous solvents appropriate for sensitive fluorescence applications in the NIR, it is necessary to understand relevant nonradiative relaxation pathways. The fluorescence properties of two representative tricarbocyanine dyes, 1,1′-bis(4-sulfobutyl)-3,3,3′,3′-tetramethyl-4,5,4′,5′-dibenzoindotricarbocyanine (IR-125) and 3,3′-bis(3-carbomethoxypropyl)-11-(diphenylamino)-10,12-ethylene-5,6,5′,6′-dibenzothiatricarbocyanine iodide (IR-132), were studied to evaluate possible solvent-dependent and solvent-independent nonradiative relaxation pathways. These dyes have extended polymethine chains and exhibit absorption and emission maxima in the NIR, with one (IR-132) possessing a reinforced structure within the heptamethine chain. The fluorescence quantum yields and lifetimes were measured in methanol, methanol/aqueous binary mixtures, and surfactant solutions, SDS (anionic surfactant), Triton X-100 (nonionic surfactant), and cetyltrimethylammonium bromide (cationic surfactant), above their CMC. Linear free energy plots were constructed from the nonradiative rate and a solvent parameter measured by an empirical scale in order to relate the efficiency of the solvent-dependent nonradiative manifold to a particular solvent characteristic. Picosecond time-resolved measurements were made on a time-correlated single photon counting (TCSPC) device which we have recently constructed using a mode-locked Ti:sapphire laser as the excitation source and a single-photon avalanche diode (SPAD) as the detector. SPADs possess large single photon detection efficiencies in the NIR and have timing responses comparable to microchannel plate photomultipliers,[30-35] making them ideal detectors for time-correlated single photon counting applications in the NIR.

(5) Strekowski, L.; Lipowska, M.; Patonay, G. *J. Org. Chem.* **1992**, *57*, 4578–4580.
(6) (a) Ernst, L. A.; Gupta, R. K.; Mujumdar, R. B.; Waggoner, A. S. *Cytometry* **1989**, *10*, 3–10. (b) Mujumdar, R. B.; Ernst, L. A.; Mujumdar, S. R.; Waggoner, A. S. *Cytometry* **1989**, *10*, 11–19. (c) Southwick, P. L.; Ernst, L. A.; Tauriello, E. W.; Parker, S. R.; Mujumdar, R. B.; Mujumdar, S. R.; Clever, H. A.; Waggoner, A. S. *Cytometry* **1990**, *11*, 418–430. (d) Mujumdar, R. B.; Ernst, L. A.; Mujumdar, S. R.; Lewis, C. J.; Waggoner, A. S. *Bioconjugate Chem.* **1993**, *4*, 105–111.
(7) West, W.; Pearce, S. *J. Phys. Chem.* **1965**, *69*, 1894–1903.
(8) Makio, S.; Kanamaru, N.; Tanaka, J. *Bull. Chem. Soc. Jpn.* **1980**, *53*, 3120–3124.
(9) Demchuk, M.; Ishchenko, A.; Mikhailov, V.; Avdeeva, V. *Chem. Phys. Lett.* **1988**, *144*, 99–103.
(10) Derevyanko, N.; Dyadyusha, C.; Ishchenko, A.; Tolmachev, A. *Teor. Eksp. Khim.* **1983**, *19*, 150–157.
(11) Buettner, A. *J. Chem. Phys.* **1967**, *46*, 1398–1401.
(12) Hofer, J. E.; Grabenstettler, R. J.; Wiig, E. O. *J. Am. Chem. Soc.* **1950**, *72*, 203–209.
(13) Mialocq, J. C.; Jaraudias, J.; Goujon, P. *Chem. Phys. Lett.* **1977**, *47*, 123–126.
(14) Tredwell, C. J.; Keary, C. M. *Chem. Phys.* **1979**, *43*, 307–316.
(15) Welford, D.; Sibbett, W.; Taylor, J. *Opt. Commun.* **1980**, *34*, 175–180.
(16) Winkworth, A. C.; Osborne, A. D.; Porter, G. *Picosecond Phenomena III*; Springer-Verlag: Berlin, 1982; pp 228–231.
(17) Arthurs, E.; Bradley, D.; Roddie, A. *Chem. Phys. Lett.* **1973**, *22*, 230–234.
(18) Kuzmin, V.; Darmanyan, A. *Chem. Phys. Lett.* **1978**, *54*, 159–163.
(19) Velsko, S.; Fleming, G. *Chem. Phys.* **1982**, *65*, 59–70.
(20) Rentsch, S. *Chem. Phys.* **1982**, *69*, 81–87.
(21) Ponterini, G.; Momicchioli, F. *Chem. Phys.* **1991**, *151*, 111–126.
(22) Fouassier, J.; Lougnot, D.; Faure, J. *Chem. Phys. Lett.* **1975**, *35*, 189–194.
(23) Kobayashi, T.; Nagakura, S. *Chem. Phys.* **1977**, *23*, 153–158.
(24) Sibbett, W.; Taylor, J.; Welford, D. *IEEE J. Quantum Electron* **1981**, *QE-17*, 500–509.
(25) Sundstrom, V.; Gillbro, T. *Chem. Phys.* **1981**, *61*, 257–269.
(26) Humphry-Baker, R.; Gratzel, M.; Steiger, R. *J. Am. Chem. Soc.* **1980**, *102*, 847–848.
(27) Sato, H.; Kawasaki, M.; Kasatani, K.; Kusumoto, Y.; Nakashima, N.; Yoshihara, K. *Chem. Lett.* **1980**, 1529–1532.
(28) Sato, H.; Kawasaki, M.; Kasatani, K.; Nakashima, N.; Yoshihara, K. *Bull. Chem. Soc. Jpn.* **1983**, *56*, 3588–3594.
(29) Turro, N.; Gratzel, M.; Braun, A. *Angew. Chem., Int. Ed. Engl.* **1980**, *19*, 675–696.
(30) Cova, S.; Longoni, A.; Andreoni, A. *Rev. Sci. Instrum.* **1981**, *52*, 408–412.
(31) Cova, S.; Longoni, A.; Ripamonti, G. *IEEE Trans. Nucl. Sci.* **1982**, *NS-29*, 599–601.

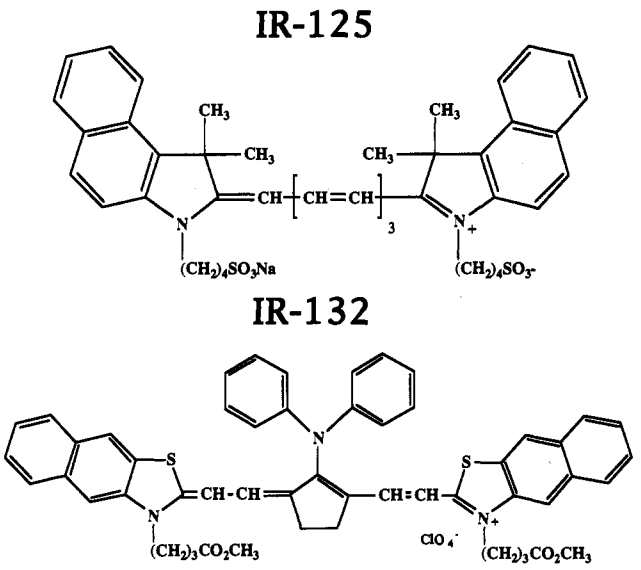

Figure 1. Chemical structures of the tricarbocyanine, NIR fluorescent dyes used in this investigation.

Experimental Section

NIR dye IR-125 was obtained from Exciton Chemical Co., Inc. (Dayton, OH), and IR-132 was obtained from Kodak chemicals (Rochester, NY). Figure 1 shows the chemical structures of these dyes. A 10^{-3} M stock solution of IR-125 in spectroscopic grade methanol (Mallinckrodt Specialty Chemicals Co., Paris, KY) and a 5×10^{-4} M stock solution of IR-132 in DMSO were prepared and stored at 5 °C. The *n*-alcohols and SDS were obtained from Mallinckrodt (Paris, KY) and Triton X-100 from Sigma Chemical Co. (St. Louis, MO). All reagents and chemicals were used as received. The dye solutions for all measurements were made daily through serial dilution of the stock solutions in the appropriate solvent and adjusted to a concentration such that the amount of methanol or DMSO in the final solution under investigation was less than 1.0%. These solutions were not purged of dissolved oxygen prior to the spectroscopic measurement. The solutions containing surfactants were maintained well above their CMC. In the neat alcohol series, all spectroscopic measurements were performed at their isoviscous temperatures in order to eliminate possible viscosity effects on the photophysics of the dyes.

The absorption spectra were acquired on a Perkin-Elmer Lambda 3B UV/vis spectrophotometer (Norwalk, CT), with the extinction coefficients calculated from the slope of a Beer–Lambert plot. The fluorescence spectra were obtained using a SPEX Fluorolog spectrofluorometer (Edison, NJ) with a 75-W xenon lamp source and a Hamamatsu R626 photomultiplier tube (Bridgewater, NJ) with a thermostated sample cell. The spectra were corrected for the wavelength-dependent throughput of the spectrometer and excited at a wavelength of 750 nm. The fluorescence quantum yields (Φ_f) were calculated relative to IR-125 in DMSO (Φ_f = 0.13)[36] using the formula[37]

$$\Phi_f = \Phi_{f,st}(F/F_{st})(\epsilon_{st}/\epsilon)(E_{st}/E)(n^2/n_{st}^2) \quad (1)$$

where F is the integrated area under the fluorescence emission profile, ϵ is the molar absorptivity of the dye at the excitation wavelength, E is the intensity of the excitation light, n is the refractive index of the solvent, and the subscript st designates those parameters associated with the secondary standard. Since the fluorescence quantum yield of the secondary standard used in this investigation can be considered provisional,[36] the quantum yields reported are intended primarily to show trends and should not be considered as absolute values.

The NIR TCSPC device consisted of a self-mode-locked Ti:sapphire laser pumped by the output of a multiline CW Ar ion laser (Coherent Lasers, Palo Alto, CA). The Ti:sapphire laser produces laser pulses at a repetition rate of 76 MHz and can be continuously tuned from approximately 760 to 870 nm with the optics set situated within the laser cavity. The temporal and spectral widths of the laser pulses were determined to be 210 fs (autocorrelation trace) and 13 nm (fwhm), respectively. The beam was focused onto a thermostated square bore sample cell with a laser diode singlet lens (Melles Griot, Irvine, CA). The laser power density used for lifetime measurements was approximately 1.3 kW cm^{-2}. The fluorescence was collected at right angles using a Nikon (Natick, MA) 40× epifluorescence microscope objective with a numerical aperture of 0.85. A Glan–Thompson polarizing prism (CVI Lasers, Albuquerque, NM) was placed within the optical train and set at the magic angle (54.7°) with respect to the polarization of the excitation light to eliminate anisotropies due to rotational diffusion. The fluorescence was imaged onto a slit serving as a spatial filter to reduce the amount of scattered photons generated at the air/glass interface of the sample cell reaching the detector. The fluorescence was further isolated from the scattering photons by an eight-cavity Fabrey–Perot interference filter (Omega Optical, Brattleboro, VT) with a center wavelength of 850 nm (fwhm = 30 nm). The fluorescence was then focused onto the photoactive area of the detector with a 6.3× microscope objective. The photodetector was a single-photon avalanche diode (EG&G Optoelectronics Canada, Vaudreuil, Canada) with a 150-μm-diameter photoactive area, which was mounted on a thermoelectric cooler and possessed dark count rates of approximately 80 counts/s. The pulses from the SPAD were amplified by a 2-GHz amplifier (Phillips Scientific, Mahwah, NJ) and conditioned with a constant fraction discriminator (CFD, Tennelec TC754, Oak Ridge, TN). The CFD pulses were directed into the gate and stop inputs of the time-to-amplitude converter (TAC, Tennelec TC863). The start input for the TAC was supplied by an intracavity diode monitoring the laser pulses and conditioned using the CFD. The fluorescence decay profiles were acquired in 4096 channels with a time resolution of 2.88 ps/channel and constructed by digitizing the output of the TAC using PCA-II hardware and software (Tennelec Nucleus, Oak Ridge, TN). The parameters describing the fluorescence decays were analyzed using a reiterative convolution nonlinear least squares method.

Table 1. Absorption Maxima and Molar Absorptivities for the NIR Dyes IR-125 and IR-132 in Various Solvent Systems

	IR-125		IR-132	
solvent	λ_{max} (nm)	$\epsilon^a \times 10^{-4}$ (cm^{-1} M^{-1})	λ_{max} (nm)	$\epsilon^a \times 10^{-4}$ (cm^{-1} M^{-1})
% H_2O^b				
0	782	19.53	811	16.35
25	782	20.31	810	12.7
50	782	22.05	809	4.37
75	781	21.12	754	2.06
ethanol	786	19.44	814	16.03
propanol	788	19.52	818	15.54
butanol	790	19.28	819	15.49
SDS	792	16.63	847	13.74
Triton	799	19.49	836	16.17

[a] The molar absorptivity was calculated at λ_{max}. [b] Represents a binary mixture consisting of water and methanol.

Results

In Table 1, the wavelength of the absorption maximum and the molar absorptivity at λ_{max} for IR-125 and IR-132 are presented in the solvent systems investigated. The absorption maximum for IR-125 and IR-132 in methanol was 782 and 811 nm, respectively. The electronic spectra of IR-125 in aqueous solvents demonstrated only a slight shift in the absorption maximum (779 nm) when compared to the methanol spectrum, while IR-132 exhibited gross changes in its spectrum. A new band appeared at 739 nm with a concomitant loss of absorption associated with the 811-nm band. For the alcohol series (methanol:ethanol: propanol:butanol), both dyes showed a progressive red-shift in the absorption maximum with increasing length in the alkyl chain of the alcohol. The addition of surfactants above the CMC to the aqueous solvent produced a large bathochromic shift in the absorption maxima for both dyes when compared to the absorption maxima observed in water. The absorption maximum for IR-

(32) Cova, S.; Longoni, A.; Andreoni, A.; Cubeddu, R. *IEEE J. Quantum Electron.* **1983**, *QE-19*, 630–634.
(33) Cova, S.; Ripamonti, B.; Lacaita, A. *Nucl. Instrum. Methods Phys.* **1987**, *A253*, 482–487.
(34) Louis, T.; Schatz, G.; Klein-Bolting, P.; Holzwarth, A.; Ripamonti, G.; Cova, S. *Rev. Sci. Instrum.* **1988**, *59*, 1148–1152.
(35) Li, Li-Q.; Davis, L. *Rev. Sci. Instrum.* **1993**, *64*, 1524–1529.
(36) Benson, R. C.; Kues, H. *J. Chem. Eng. Data* **1977**, *22*, 379–383.
(37) Demas, J.; Crosby, G. *J. Phys. Chem.* **1971**, *75*, 991–1024.

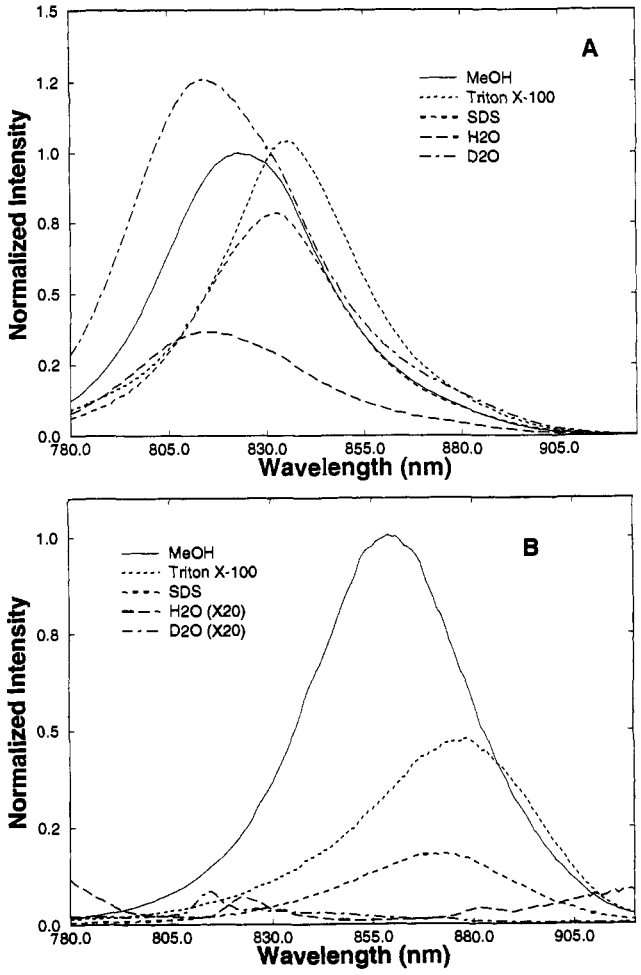

Figure 2. Fluorescence emission spectra of IR-125 (A) and IR-132 (B) in various solvent systems. The spectra were obtained with an excitation wavelength of 750 nm and were corrected for the wavelength-dependent throughput of the spectrometer. All spectra were normalized to the emission maximum in methanol.

125 in water appeared at 779 nm and shifts to 792 nm in SDS and 799 nm in Triton X-100. For IR-132, the absorption maximum in water was at 739 nm and shifts to 847 nm in SDS and 836 nm in Triton X-100. The addition of a cationic surfactant (cetyltrimethylammonium bromide) above the CMC resulted in no observable changes in the spectra of these dyes when compared to the aqueous spectra. No differences in the absorption spectra for IR-125 and IR-132 in H_2O and D_2O were observed.

Figure 2 shows the fluorescence emission profiles for these dyes in methanol, H_2O, D_2O, SDS, and Triton X-100. Inspection of the profiles for IR-125 indicated a decrease in the emission intensity in H_2O when compared to methanol with an associated blue-shift in the emission maximum. For D_2O, the emission intensity was seen to increase substantially when compared to H_2O. In the surfactant solutions, the emission maxima shifted to longer wavelengths, and the Triton X-100 solution demonstrated a slight increase in intensity, while SDS showed a slight decrease when compared to the methanol spectrum. For IR-132, a dramatic decrease in the emission intensity for the aqueous solvent was observed when compared to methanol with the addition of either surfactant above the CMC restoring some of the fluorescence emission. The addition of the cationic surfactant did not alter the emission intensity for both dyes when compared to the pure aqueous solvent. No difference in the emission intensity was observed for IR-132 in D_2O when compared to H_2O. In binary mixtures of water/methanol, the general shapes of the spectra for these dyes did not change as a function of added water, but did show a decrease in the intensity as the concentration

Table 2. Photophysical Properties of the NIR Dye IR-125 in Various Organic Alcohols, D_2O, H_2O/Methanol Binary Mixtures, Surfactant Solutions, and Methanol/Glycerol Solvents (Numbers in Parentheses are the χ^2 Values Associated with the Fitted Lifetime Function and the Experimental Data)

solvent	Φ_f[a]	τ_f[b] (ns)	k_r (ns^{-1})	k_{nr} (ns^{-1})	k_r[c] (ns^{-1})
% H_2O					
0	0.04	0.47 (1.3)	0.09	2.0	0.10
25	0.04	0.34 (1.4)	0.11	2.8	0.12
50	0.02	0.22 (1.5)	0.11	4.4	0.13
75	0.02	0.16 (6.0)	0.12	6.1	0.10
100	0.01	*d*	*d*	*d*	*d*
ethanol	0.05	0.57 (1.4)	0.10	1.7	0.12
propanol	0.06	0.69 (3.0)	0.09	1.4	0.10
butanol	0.07	0.72 (3.0)	0.10	1.3	0.10
SDS	0.05	0.34 (1.4)	0.15	2.8	0.13
Triton	0.06	0.57 (1.6)	0.11	1.7	0.12
D_2O	0.06	0.60 (4.7)	0.11	1.6	0.10
% glycerol[e]					
0 (0.59)		0.47 (1.3)			
20 (1.29)		0.49 (1.3)			
40 (4.36)		0.50 (1.3)			
80 (89.12)		0.52 (1.3)			

[a] The relative standard deviation in all quantum yield measurements was found to range from 10 to 20%, as determined from three replicate measurements in each particular solvent system. [b] The relative standard deviation in all fluorescence lifetime determinations ranged from 1 to 3%. [c] Radiative rates calculated using the Strickler–Berg relationship. [d] Lifetime could not be determined with the resolution of the NIR TCSPC device. [e] Glycerol/methanol binary solvents with the viscosity (cP) of the mixture at 25 °C shown in parentheses.

Table 3. Photophysical Properties of the NIR Dye IR-132 in Various Organic Alcohols, D_2O, H_2O/Methanol Binary Mixtures, Surfactant Solutions, and Methanol/Glycerol Solvents (Numbers in Parentheses are the χ^2 Values Associated with the Fitted Lifetime Function and the Experimental Data)

solvent	Φ_f[a]	τ_f[b] (ns)	k_r (ns^{-1})	k_{nr} (ns^{-1})	k_r[c] (ns^{-1})
% H_2O					
0	0.07	0.70 (1.4)	0.10	1.3	0.10
25	0.06	0.59 (1.1)	0.09	1.6	0.10
50	0.04	0.52 (1.1)	0.07	1.8[d]	0.01
75	0.005	0.41 (1.9)	0.01	2.4[d]	0.04
100	*e*	*e*	*e*	*e*	*e*
ethanol	0.09	0.76 (1.5)	0.12	1.2	0.11
propanol	0.10	0.88 (3.0)	0.12	1.0	0.11
butanol	0.11	0.91 (4.0)	0.12	0.98	0.11
SDS	0.03	0.75 (3.1)	0.04	1.3	0.10
Triton	0.07	0.63 (3.1)	0.11	1.5	0.12
D_2O	*e*	0.71 (25.6)[f]	*e*	*e*	*e*
% glycerol					
0		0.70 (1.4)			
20		0.68 (1.2)			
40		0.65 (1.0)			
80		0.57 (1.9)			

[a] The relative standard deviation in all quantum yield measurements was found to range from 10 to 20%, as determined from three replicate measurements for each particular solvent system. [b] The relative standard deviation in all fluorescence lifetime determinations ranged from 1 to 3%. [c] Radiative rates calculated using the Strickler–Berg relationship. [d] Calculated assuming that $k_r = 0.10 \times 10^9\ s^{-1}$. [e] The low emission intensity exhibited in the solvent did not permit calculation of this photophysical parameter. [f] The large χ^2 resulted from a significant amount of scattering photons in the decay profile.

of water was increased as well as a slight blue-shift in the emission maximum. In the alcohol series, both dyes showed emission intensities that progressively increased with a corresponding red-shift in the emission maximum as the alkyl chain length in the alcohol was increased.

In Table 2 the fluorescence quantum yields for IR-125 are presented, and in Table 3 the values for IR-132 are shown for the various neat and binary solvent systems investigated. In the binary H_2O/methanol mixtures, the quantum yields for both dyes increased as the percentage of H_2O was decreased, with IR-132 demonstrating a larger net decrease in Φ_f between

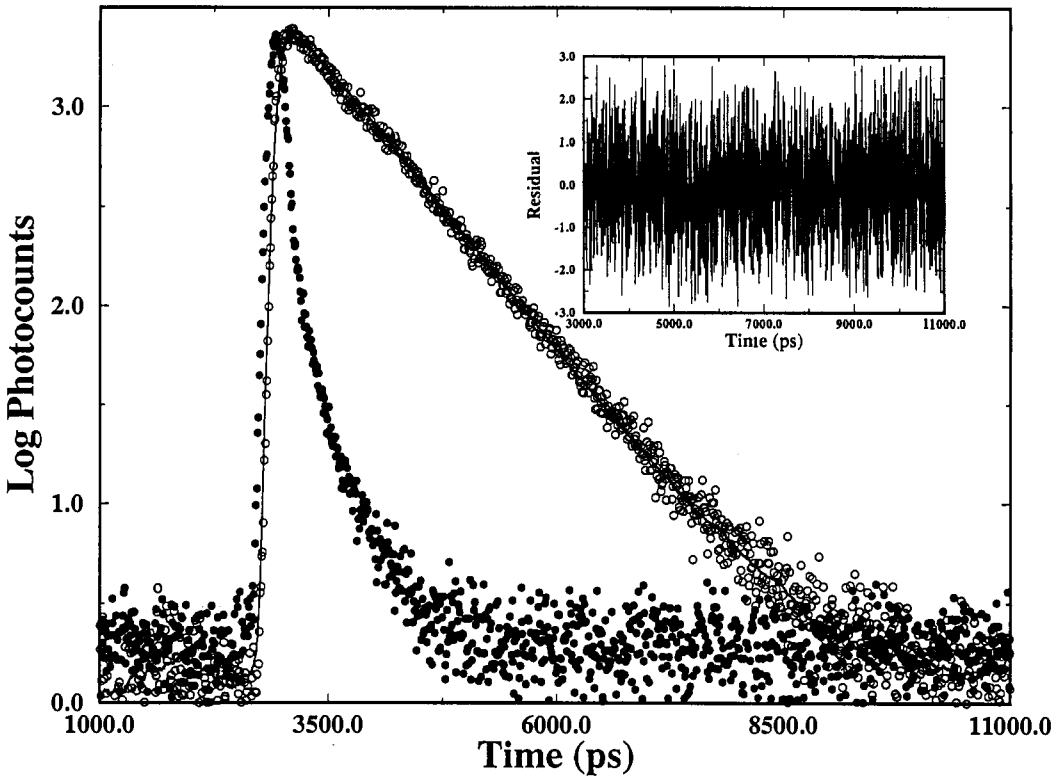

Figure 3. Fluorescence decay profile (open circles) for IR-125 in ethanol and instrument response function (filled circles) using the time-correlated NIR fluorescence spectrometer. The solid line represents the best fit function to the data, and the weighted residuals are shown in the inset.

methanol and H_2O/methanol (75/25). For the *n*-alcohol series, the quantum yields showed only slight increases as the length of the alkyl chain associated with the *n*-alcohol was increased, with Φ_f increasing from 0.04 and 0.07 in methanol to 0.07 and 0.11 in butanol for IR-125 and IR-132, respectively. The addition of SDS and Triton surfactants above their CMCs increased the fluorescence quantum yields for IR-125 and IR-132 when compared to the quantum yields in the pure aqueous solutions. In the case of the cationic surfactant, IR-125 and IR-132 displayed Φ_f values similar to that observed in the pure aqueous solvent.

In Tables 2 and 3 the fluorescence lifetimes (τ_f) for these NIR dyes are also shown. A typical decay profile for IR-125 in methanol along with the instrument response function and the weighted residuals are shown in Figure 3. In all cases examined, the decays were adequately fit by a single-exponential function. Attempts to fit the data to a double-exponential function did not increase the goodness of the fit, as indicated by the value of χ^2. In the H_2O/methanol binary solvents, the lifetimes were found to show large decreases as the percentage of H_2O was increased. For IR-125, τ_f was 0.47 ns in 100% methanol, and in H_2O/methanol (75/25), τ_f was 0.16 ns. For IR-132, the lifetime was 0.70 ns in methanol, while for H_2O/methanol (75/25), τ_f decreased to 0.41 ns. In the alcohol series, τ_f slightly increased for both dyes as the alkyl chain length was increased. The fluorescence lifetimes for IR-125 and IR-132 were also found to be dramatically longer in the deuterated solvent when compared to the lifetimes in H_2O/methanol (75/25). The lifetimes of both dyes in the micellar media were also longer when compared to those exhibited in the water/methanol (75/25) binary solvent system.

The effects of solution viscosity (η) on the fluorescence lifetimes associated with these dyes were determined in methanol/glycerol binary mixtures, since these solvents have nearly the same polarity, but show large differences in their room temperature viscosities (954 cP for glycerol and 0.597 cP for methanol). Figure 4 shows a plot of log τ_f vs log η for IR-125 and IR-132. The slopes of these plots indicated an $\eta^{0.02}$ dependence (IR-125) and an $\eta^{-0.04}$ dependence (IR-132) of τ_f on solution viscosity.

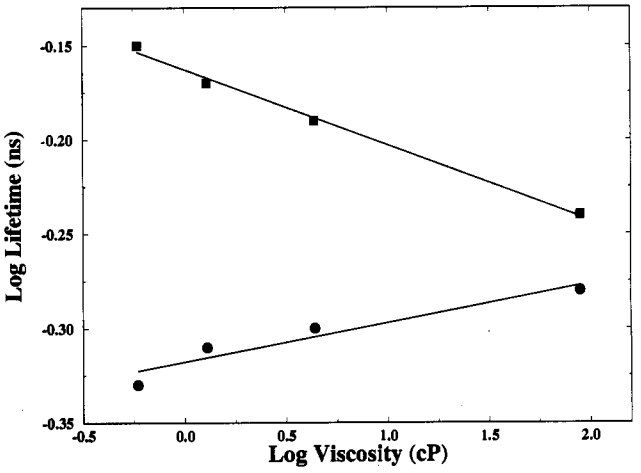

Figure 4. Log τ_f versus log η for IR-125 (circles) and IR-132 (squares). A linear regression analysis of this data indicated a slope of 0.02 (r = 0.95) for IR-125 and –0.04 (r = 0.99) for IR-132.

The radiative (k_r) and the nonradiative (k_{nr}) decay rates for a quasi-two-level system can be calculated from the fluorescence quantum yield and lifetime using

$$k_r = \Phi_f/\tau_f \tag{2}$$

$$k_{nr} = (1 - \Phi_f)/\tau_f \tag{3}$$

Radiative rates for these dyes are shown in Tables 2 and 3. For a consistency check, the radiative rates were also calculated from the absorption and emission spectra using the Strickler–Berg relationship:[38]

$$k_r = (2.88 \times 10^{-9})n^2\langle\tilde{\nu}_f^{-3}\rangle(g_l/g_u)\int \epsilon \, d \ln \tilde{\nu} \tag{4}$$

where n is the refractive index of the given solvent, $\langle\tilde{\nu}_f^{-3}\rangle$ is obtained from the integration of the fluorescence emission spectrum and

(38) Strickler, S.; Berg, R. *J. Chem. Phys.* **1962**, *37*, 814–822.

the integration of the same spectrum multiplied by the cubed intensity value at each frequency, g_l/g_u represents the degeneracy in the excited and ground electronic states, and $\int \epsilon \, d \ln \tilde{\nu}$ is the integrated molar absorptivity over the electronic absorption band. The values of k_r for IR-125 and IR-132 as calculated from the Strickler–Berg relationship are in good agreement with those values determined using the experimental quantum yields and lifetimes for the alcohol series. The radiative rates were found in the range $(0.10–0.12) \times 10^9$ s^{-1} for IR-125, with similar values for IR-132 in the neat alcohols. In the H_2O/methanol binary solvents, fair agreement between the Strickler–Berg radiative rates and those calculated from Φ_f and τ_f for IR-125 was observed. For IR-132, poor agreement was found at the higher percentages of water.

The nonradiative rates for IR-125 and IR-132 in the neat alcohol series showed slight decreases when the alkyl chain length of the alcohol was increased. For IR-125, k_{nr} increased as the percentage of water in the H_2O/methanol binary mixture was increased ($k_{nr} = 2.8 \times 10^9$ s^{-1} in 25% H_2O and $k_{nr} = 6.1 \times 10^9$ s^{-1} in 75% H_2O). If the radiative rates for the primary fluorescent species of IR-132 do not significantly change in the H_2O/methanol series, changes in τ_f should reflect changes in the nonradiative rate, with the approximate nonradiative rate determined from $1/\tau_f - k_r$. As can be seen from Table 3, the calculated k_{nr} values for IR-132 increase with increasing water composition, but show a smaller net change in the nonradiative rate between methanol and 75/25 water/methanol when compared to IR-125.

Discussion

The progressive red-shift in the absorption maximum for IR-125 and IR-132 as a function of alkyl chain length in the alcohol series is consistent with previous research on polymethine dyes, which attributed the bathochromic shift in the absorption maximum to nucleophilic solvation of the cationic center of the dye.[10] Solvation results in a lowering of the excited-state energy as Hückel calculations show that the positive charge is more localized in the excited state,[9] making it more susceptible to nucleophilic solvation. In the alcohol series methanol:ethanol:propanol:butanol the nucleophilicity of the solvent increases with increasing alkyl chain length, giving rise to the observed bathochromic shift. Since methanol is a better nucleophile than water, the binary H_2O/methanol mixtures should yield a blue-shift in the absorption maximum with increasing water concentration, consistent with the observed data.

Many polymethine dyes form aggregates in aqueous solvents, with longer polymethine chains yielding a greater tendency to aggregate.[8] For IR-132, aggregation is clearly evident from inspection of the ground-state spectra in H_2O and methanol. If it is assumed that the dye exists predominately in the monomeric form in methanol, the absorption band for IR-132 at 739 nm can be assigned to a dimer or other higher order aggregates, while the band at 811 nm is associated with the monomeric form of the dye. In the case of IR-125, no apparent aggregation was observed, since the general shape of the spectra in H_2O and methanol was similar, the only difference being the slight blue-shift in the absorption maximum for H_2O. The lack of aggregation for this dye in aqueous solvents most likely arises from the negatively charged sulfonic groups on the dye, providing the dye with a better sphere of solvation.

Since solvents of increasing nucleophilicity cause a bathochromic shift in the absorption maximum, the shift in the absorption maxima to longer wavelengths by the addition of surfactants above their CMC to the aqueous solvent implies effective partitioning of both dyes into the hydrophobic cavity of the anionic and nonionic micelles, where the dye is shielded from the poor nucleophilic interstitial water solvent. The lack of an observable absorption band in the SDS spectrum for IR-132 at 739 nm indicates that the majority of the dye molecules reside within the hydrophobic cavity of the micelle in a monomeric form at this surfactant concentration. The lack of changes in the absorption spectra for these dyes in the cationic surfactant when compared to the pure aqueous spectra indicates that these dyes do not partition into the hydrophobic core of this particular micelle system.

Calculation of the radiative and nonradiative rates showed that the radiative rate for the most part was insensitive to the nature of the solvent. The differences in the radiative rates for IR-132 between the alcohol series and the water/methanol binary mixtures at the higher percentages of H_2O result from interrogation of various ground-state species at the excitation wavelength used to obtain the emission profiles. Significant changes in the electronic spectra support this conclusion. The measured quantum yield at high percentages of water, therefore, represents a combined yield of the monomeric and various aggregate forms of the dye. The nonradiative rates for these dyes showed only small changes in the alcohol series, with larger changes observed in the water/methanol binary solvents. The nonradiative rate, which represents a sum of rates associated with different processes which serve to depopulate the excited state, can be represented in many tricarbocyanine dyes by

$$k_{nr} = k_{isc} + k_p + k_{ic} + k_{sd} \qquad (5)$$

where k_{isc} is the rate associated with intersystem crossing, k_p is the photoisomerization rate, k_{ic} represents the rate of internal conversion (including the time-dependent component), and k_{sd} is a solvent-dependent nonradiative rate. The time-dependent k_{ic} arises from conformational changes which occur during the excited-state lifetime which distort the planarity of the molecule and affect the rate of internal conversion. The rate of photoisomerization and the time-dependent internal conversion rate can exhibit a solvent viscosity dependence since molecular reorganization during the excited-state lifetime is necessary. In isoviscous solvents, differentiation between k_{sd} and the viscosity-dependent rates can be made. The intersystem crossing rate can be affected by the amount of dissolved oxygen present in the solvent system, but previous research has shown that in the absence of intra- or intermolecular heavy atoms, the rate of intersystem crossing is small in di- and tricarbocyanine dyes.[16,39–41]

The small viscosity dependence on the fluorescence lifetimes observed for IR-125 (see Figure 4) in the glycerol/methanol binary mixtures implies that extensive conformational reorganization in the excited state does not occur for this extended-polymethine dye. The short upper-state lifetime coupled with the extended length of the polymethine chain may preclude the conformational changes necessary for cis/trans isomerization to occur during the time scale of the excited state (small or negligible k_p). The lack of a second component arising from a photoisomer in the fluorescence decay profiles supports this supposition. The present results for IR-125 are consistent with previous research on cis/trans photoisomerization which showed that the activation energy for cis/trans photoisomerization was greater in the dicarbocyanines when compared to the carbocyanines due to less steric hindrance between the heteroaromatic rings in dicarbocyanine dyes.[18] Since IR-125 is a tricarbocyanine dye, steric hindrance between the heteroaromatics is minimal and should result in a larger activation energy for cis/trans photoisomerization. However, transient absorption measurements on the tricarbocyanine dye HITCI (1,1′,3,3,3′,3′-hexamethylindotricarbocyanine iodide) demonstrated the existence of a photoisomer.[22] The additional aromatic ring on each heteroaromatic fragment of IR-125 increases the viscous drag and is sufficient to inhibit the isomerization of the dye during its upper-state lifetime. IR-125 does show a slight dependence of τ_f on viscosity, which may arise

(39) Cooper, W.; Liebert, N. *Photogr. Sci. Eng.* **1972**, *16*, 25.
(40) Cooper, W.; Rome, K. *J. Phys. Chem.* **1974**, *78*, 16–21.
(41) Andrews-Wilberforce, D.; Patonay, G. *Appl. Spectrosc.* **1989**, *43*, 1450–1455.

Table 4. Solvent $E_T(30)$ and B_{KP} Values Used in this Study

solvent	$E_T(30)^a$ (kcal/mol)	B_{KP}^b (cm^{-1})
methanol	55.5	218
ethanol	51.9	235
propanol	50.7	236
butanol	50.2	231
% H_2O		
25	56.9	
50	58.3	
75	60.3	
SDS	57.5	
Triton	53.0	

[a] Taken from ref 45. The $E_T(30)$ values for SDS and Triton were taken from ref 47. [b] Taken from ref 46.

from partial rotation of the heteroaromatic terminal groups from the molecular plane during the excited state, giving rise to a time-dependent rate of internal conversion.[15]

In the case of IR-132, the negative viscosity dependence is a consequence of the increased $E_T(30)$ value (see below for discussion of $E_T(30)$ values) of this binary mixture when the percentage of glycerol is increased and indicates that molecular conformational changes do not occur during the excited-state lifetime (negligible k_p). The reinforcement in the structure of the dye within the heptamethine chain minimizes and/or eliminates conformational reorganization and aids in preserving ground-state conformations during the excited-state lifetime.

Decreases in the nonradiative rates for IR-125 and IR-132 in the micelle solutions when compared to the pure aqueous solvent is a result of changes in the microenvironment associated with the interior of the micelle. These changes include a higher viscosity, lower dielectric constant and polarity, poorer hydrogen bond donor capabilities, and better nucleophilicity when compared to the interstitial solution. The negligible viscosity dependence on the fluorescence lifetimes for these dyes indicates that increased solution viscosity in the micellar core is not responsible for the favorable fluorescence properties observed in the micelle solutions and depends upon another solvent parameter associated with the interior of the micelle.

In order to evaluate the efficacy of predicting the rate of this solvent-dependent nonradiative process (k_{sd}) with a characteristic associated with the solvent, linear free energy relationships were constructed from ln k_{nr} versus a specific solvent parameter. The slope of such a plot represents the sensitivity of the nonradiative pathway to a particular property of the solvent.[42,43] Plots were constructed using the empirical $E_T(30)$ scale[44,45] and the solvent basicity scale (B_{KP}).[46] The $E_T(30)$ value depends strongly on the dipolarity/polarizability and hydrogen bond donor (HBD) capabilities of the solvent. The B_{KP} solvent parameter indicates the solvent's nucleophilic capabilities (hydrogen bond acceptor, HBA), with larger numbers indicative of better nucleophilic solvents. In Table 4, the $E_T(30)$ and B_{KP} values of the solvents used in this study are shown.

Free energy plots using the $E_T(30)$ solvent parameter scale for both dyes are shown in Figure 5. Linear relationships were obtained with good correlation coefficients for both dyes in the alcohol and H_2O/methanol series with a discontinuity in the plots between the alcohol series and the H_2O/methanol binary mixtures. In the alcohol series, the slopes of these plots were small. For the H_2O/alcohol series, the slopes of these plots increased, with the value for IR-125 nearly 2-fold greater than that associated

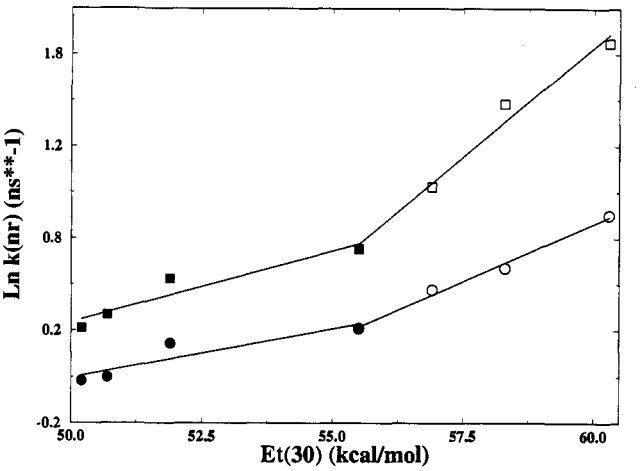

Figure 5. Linear free energy plots of ln k_{nr} versus solvent $E_T(30)$ value in *n*-alcohols (filled symbols) and H_2O/methanol (open symbols) for IR-125 (squares) and IR-132 (circles). The solid lines were determined from a linear regression analysis of the data. The slopes of these plots were 0.08 (r = 0.99) and 0.05 (r = 0.91) for IR-125 and IR-132, respectively, in the alcohol series and in the H_2O/methanol systems, 0.24 (r = 0.99) for IR-125 and 0.13 (r = 0.99) for IR-132. The temperatures of the solvent systems were adjusted to yield isoviscous solutions to minimize possible viscosity dependencies on the nonradiative rate.

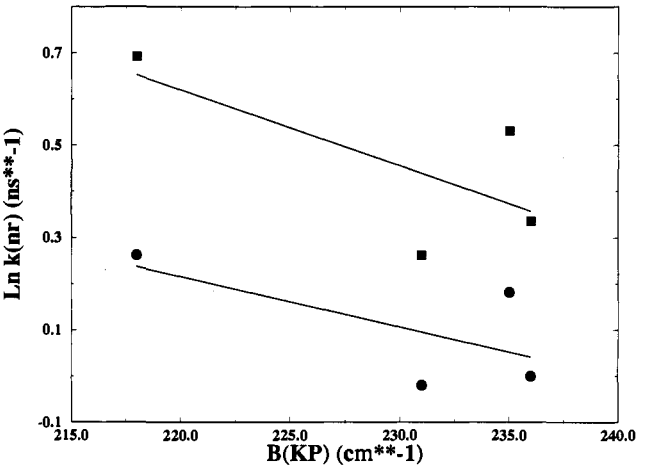

Figure 6. Linear free energy plots of ln k_{nr} versus solvent B_{KP} value in the *n*-alcohol series for IR-125 (squares) and IR-132 (circles). A linear regression analysis of the data yielded slopes of –0.01 (r = 0.65) for IR-125 and –0.02 (r = 0.79) for IR-132.

with IR-132. The greater sensitivity of k_{sd} toward H_2O exhibited by IR-125 is somewhat surprising, because the quantum yield of IR-132 demonstrated larger changes when the amount of H_2O in the binary mixture was increased. Since the decay profile of IR-132 could adequately be described by a single-exponential function, only a single species constitutes the measured lifetime, most likely the monomeric species since at the low dye concentrations used to measure the fluorescence lifetimes the monomeric species should be the dominant form. The net changes in the lifetimes observed for IR-132 in the H_2O/methanol series were similar to that of IR-125, while the quantum yields for this same series were dramatically greater in the case of IR-132. This is a consequence of the fact that the experimentally determined quantum yield represents a weighted average of the fluorescence efficiency of the monomer and the various aggregate forms of the dye. These results indicate that k_{sd} associated with the monomeric form of IR-132 is less sensitive to the polarity and/or HBD capabilities of the solvent when compared to IR-125, which is not apparent through simple inspection of the quantum yields.

In Figure 6, ln k_{nr} versus the solvent's nucleophilicity as indicated by the empirical B_{KP} scale is shown for the alcohol series. As can be seen, increasing nucleophilicity of the solvent

(42) Hicks, J.; Vandersall, M.; Babarogic, Z.; Eisenthal, K. *Chem. Phys. Lett.* **1985**, *116*, 18–24.
(43) Hicks, J.; Vandersall, M.; Sitzmann, E.; Eisenthal, K. *Chem. Phys. Lett.* **1987**, *135*, 413–420.
(44) Reichardt, C. *Angew. Chem., Int. Ed. Engl.* **1979**, *18*, 98–110.
(45) Reichardt, C. *Molecular Interactions*; John Wiley and Sons: New York, 1982; Vol. 3, pp 241–282.
(46) Koppel, A.; Paju, A. *Org. React.* **1976**, *11*, 121–125.
(47) Zacharlasse, K.; Phuc, N.; Kozanklewicz, B. *J. Phys. Chem.* **1981**, *85*, 2676–2683.

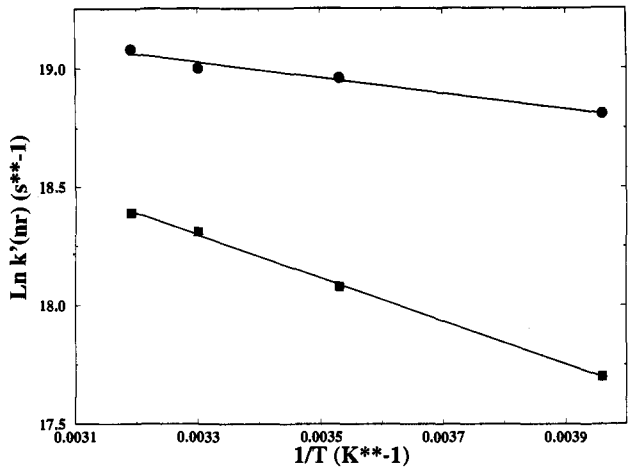

Figure 7. Arrhenius plots of the nonradiative rate corrected for solvent polarity (k') versus $1/T$ in the alcohol series methanol:ethanol:propanol: butanol for IR-125 (squares) and IR-132 (circles). A linear regression analysis yielded an activation energy of 2.6 kcal/mol for IR-125 (r = 0.96) and 1.6 kcal/mol for IR-132 (r = 0.94). The temperature was adjusted in each solvent such that the viscosity of the solutions was constant.

resulted in *decreased* nonradiative rates for both dyes in the alcohol series, with similar slopes and also poorer correlation coefficients than those found in the $E_T(30)$ plots. The red-shift in the emission and absorption maxima indicates stabilization of the excited state with increasing solvent nucleophilicity, although this solvation process is not the major solute–solvent interaction that results in the solvent-dependent quenching of these dyes.

The energy (E_a) associated with an activated process (nonradiative manifold) can be obtained from an Arrhenius-type plot, constructed from the nonradiative rates in the alcohol series which were obtained at various temperatures to maintain a constant viscosity. Since both dyes demonstrated a dependence of the nonradiative rate on solvent polarity and/or HBD ability, a correction term in the nonradiative rate must be included to account for this dependency.[42,43] The corrected rate constant (k') is obtained from

$$k' = k_{nr}e^{-[A(E_T(30)-30)]/RT} \quad (6)$$

where A is the sensitivity of the nonradiative rate to the solvent's polarity (slope in the plots of Figure 5). The Arrhenius plots for IR-132 and IR-125 are shown in Figure 7. Evaluation of the slopes indicated an activation energy of 2.6 kcal/mol for IR-125 and 1.6 kcal/mol for IR-132.

In the longer chain alcohols, where aggregation is not present and the $E_T(30)$ value of the solvent is small (low k_{sd}), the quantum yields for these dyes were below 15% and the fluorescence lifetimes were less than 1 ns, indicating the presence of an additional nonradiative manifold. A negligible rate of intersystem crossing and photoisomerization implicates internal conversion as a major nonradiative relaxation pathway. The rate of an internal conversion process, which involves quantum mechanical tunneling from the lowest vibrational level of the excited singlet state to an excited vibrational level of the ground electronic state, can be estimated from the expression[48]

$$k_{ic} = (2\pi/\hbar)\rho_E\beta_E\sum\langle\phi_v|\phi_i\rangle^2 \quad (7)$$

where ρ_E is the density of states, β_E is the electronic factor for the radiationless transition, and $\sum\langle\phi_v|\phi_i\rangle^2$ is the Franck–Condon factor, which accounts for the overlap between the vibrational levels ϕ_v and ϕ_i. The factors ρ_E and β_E depend upon the ground-state properties of the dyes and are typically constants for a given dye, while the Franck–Condon overlap term may show time dependency if conformational changes occur in the molecule during the excited-state lifetime. For visible fluorescent dyes, internal conversion is negligible, due to the large energy gap between electronic levels (small β_E). In the NIR dyes, smaller energy gaps between electronic levels lead to larger rates of internal conversion. Previous work has indicated a negative exponential dependence on the rate of internal conversion with the energy between electronic levels involved in the transition.[49] In addition, the conformationally nonrigid polymethine chain in the NIR dyes leads to more vibrational degrees of freedom (larger ρ_E term) when compared to the visible fluorescent dyes. Inspection of the molecular structures shows that IR-132 has a bridging unit within the heptamethine chain, while IR-125 does not, suggesting a more rigid and planar molecule, giving rise to lower rates of internal conversion due to a reduced number of vibrational degrees of freedom and thus larger quantum yields and longer lifetimes. The nonradiative rate for IR-125 in butanol was found to be 1.3 ns^{-1}, while for IR-132 k_{nr} was 0.98 ns^{-1}, indicating a possible higher rate of internal conversion in IR-125. Support of this conclusion would require careful measurement of the intersystem crossing rates in these dyes. The D_2O results also support the existence of an efficient internal conversion process, since this nonradiative pathway shows a heavy isotope effect.[50] The lifetimes of both dyes were found to be significantly longer in the deuterated solvents when compared to the protium solvent. In the case of IR-132, the quantum yields were comparable in H_2O and D_2O, while the quantum yield for IR-125 was higher in D_2O. Major changes in the electronic spectra for IR-132 in D_2O and H_2O indicate similar tendencies to form aggregates in both solvents, yielding no observable increase in the fluorescence quantum yield for D_2O. The lifetime for IR-132, which was measured in dilute solutions where aggregation is minimal, indicated a sizeable increase in the lifetime for D_2O when compared to H_2O.

Conclusions

From the photophysical properties of the representative NIR dyes measured in this investigation, several structural constraints warrant consideration in the synthetic preparation of new tricarbocyanine fluorochromes appropriate for applications which demand high sensitivity. While others may be important in the design of NIR dyes with favorable fluorescence efficiencies, the major constraints resulting from the present investigation include the following:

1. Incorporating Charged Groups on the Chromophore. The inclusion of charged groups prevents the self-aggregation of the hydrophobic dyes in aqueous solvents, which occurs even at relatively low dye concentrations. The aggregation process results in gross changes in the absorption spectra, shifting the absorption maxima from the NIR into another region of the spectrum. In addition, the aggregates fluoresce with much lower efficiencies than the monomeric form of the dye. Several researchers have shown that conjugation of NIR dyes to highly charged molecules, for example antibodies, can inhibit the aggregation process as well.[6]

2. Inclusion of Large Heteroaromatic Units in the Terminal Groups. Larger heteraromatic fragments linked by the polymethine chain increase the viscous drag and inhibit conformational reorganization during the electronic transition and the excited-state lifetime, minimizing the efficiency of the internal conversion process and resulting in reduced or negligible rates of photoisomerization.

3. Insertion of Bridging Units in the Polymethine Chain. Bridging units or structural reinforcement within the polymethine chain decreases the number of vibrational degrees of freedom in the molecule, which helps to reduce the rate of internal conversion. In addition, the bridging units can impede conformational reorganization during the excited-state lifetime, reducing or

(48) Phillips, D. *Photochemistry* **1970**, *1*, 8.

(49) Martin, M. *Chem. Phys. Lett.* **1975**, *35*, 105–111.

(50) Siebrand, W.; Williams, D. F. *J. Chem. Phys.* **1968**, *49*, 1860–1871.

eliminating nonradiative photoisomerization or the time-dependent component of internal conversion. Drastic fluorescence enhancement in the carbocyanine dye 1,1′-diethyl-2,2′-cyanine iodide has been observed when an ethylene or methylene bridging unit is placed between the 1,1′ nitrogen heteroatoms, restricting the molecule to a more planar conformation during the excited-state lifetime, lowering the efficiency of the internal conversion process.[14]

4. Avoiding Heavy Atoms within the Molecule Structure. We have collected preliminary data which has shown that heavy atoms, for example halogens, can severely reduce the fluorescence lifetime and quantum yield of the dye when inserted directly on the chromophore due to increased intersystem crossing arising from enhanced spin orbit coupling.

5. Use of Organized Media or Deuterated Solvents in the Fluorescence Analysis. The use of organized media or deuterated solvents can minimize the nonradiative manifold which is dependent upon the polarity and/or HBD capabilities of the solvent. Although this is not a structural design constraint, it is an effective tool at maximizing the fluorescence efficiency of the NIR fluorochrome when used in a particular application.

On the basis of the photophysical properties of IR-132 and IR-125, insertion of bridging units within the polymethine chain and the use of nonaqueous solvents are logical approaches to reducing the nonradiative efficiencies of these dyes. The relative importance of the aforementioned design constraints in determining the fluorescence efficiency of any particular tricarbocyanine dye should be evaluated on a case-by-case basis. For example, while many tricarbocyanine dyes may display a solvent-dependent nonradiative rate, the magnitude of this will vary, as seen in the results for IR-125 and IR-132. However, some generalizations concerning nonradiative pathways in the tricarbocyanine dyes can be made, the major one being a larger rate of internal conversion when compared to the visible fluorescent dyes due to the smaller energy difference between the ground and first excited singlet state. In critical applications, the use of deuterated solvents can enhance the fluorescence efficiency, thereby increasing the sensitivity of the measurement since it reduces the rate of the internal conversion process.

Acknowledgment. The authors would like to thank Coherent Lasers for supplying the argon ion laser. Partial financial support of this research by the Louisiana Educational Quality Support Fund (LEQSF) is deeply appreciated. The authors would also like to thank Prof. Hammer for helpful discussions during the course of this work and Prof. Maverick for the use of the steady-state fluorescence spectrometer.